OPEN ACCESS
International Journal of Innovations in Science & Technology

Comparative Assessment of Object-Based and Pixel-Based Approaches for Crop Cover Classification

Amara Sattar[1], Syed Muhammad Irteza[2], Sawaid Abbas[1,3,*], Sami Ullah Khan[4], Muhammad Usman[5]

[1]Smart Sensing for Climate and Development, Center for Geographical Information System, University of the Punjab, Lahore, Pakistan

[2]Punjab Information Technology Board, Lahore, Pakistan

[3]Department of Land Surveying and Geo-Informatics, The Hong Kong Polytechnic University, Hong Kong SAR

[4]Urban Unit, Lahore

[5]Interdisciplinary Research Center for Aviation and Space Exploration, King Fahd University of Petroleum and Minerals, Dhahran, Saudi Arabia

[*]**Correspondence:** sawaid.gis@pu.edu.pk (S.A); sawaid.abbas@connect.polyu.hk

Citation | Sattar. A, Irteza. S. M, Abbas. S, Khan. S. U, Usman. M "Comparative Assessment of Object-Based and Pixel-Based Approaches for Crop Cover Classification", IJIST, Special Issue pp 257-269, June 2024

Received | June 02, 2024 **Revised |** June 07, 2024 **Accepted |** June 11, 2024 **Published |** June 16, 2024.

Introduction/Importance of Study: Accurate crop identification and classification are crucial for effective agro-based planning and ensuring food availability. Reliable classification helps optimize agricultural productivity and resource management.

Novelty Statement: This study innovatively compares pixel-based and object-based approaches for machine learning-oriented classification methods to develop crop-type maps in Rahim Yar Khan, Pakistan.

Material and Method: Utilizing the Google Earth Engine (GEE) cloud computing platform, pre-processing steps were applied to Synthetic Aperture Radar Sentinel-1 and Sentinel-2 data. Integration of Sentinel-1 (VV, VH) and Sentinel-2 satellite bands enabled the computation of various indices and the production of composite images for subsequent analysis. The primary objective was to evaluate the effectiveness of these approaches in classifying major crops: cotton, rice, and sugarcane. Time-specific images were employed to leverage crop seasonality; for instance, an August composite image was prioritized for cotton, while September composites were used for rice and sugarcane classification. The study utilized two object-based segmentation approaches: Simple Non-Iterative Clustering (SNIC) on the GEE platform and Object-Based Image Analysis (OBIA) using Multi-Resolution Segmentation in E-Cognition software. The Random Forest (RF) machine learning algorithm was applied to both pixel-based and object-based approaches. Field sample data, including cotton, rice, sugarcane, orchards, and other crops, were used for classification, validation, and accuracy assessment. A comparative analysis was conducted to evaluate the performance of pixel-based and object-based methods.

Result and Discussion: The RF algorithm applied to pixel-based approaches using Sentinel-1 and Sentinel-2 imagery bands with composite indices demonstrated superior results. The pixel-based RF classification achieved 98% accuracy with a kappa coefficient of 92%. In comparison, RF applied to SNIC in GEE achieved 96% accuracy with a kappa coefficient of 95%, while OBIA in E-Cognition attained an accuracy of 89%.

Concluding Remarks: The study concludes that tuning the segmentation parameters in both E-Cognition and SNIC algorithms can enhance the accuracy of object-based classification.

Keywords: Sentinel-1, Sentinel-2, Google Earth Engine (GEE), Random Forest (RF), Simple Non-Iterative Clustering (SNIC), Vegetation Indices, Crop classification, Object Based Image Analysis (OBIA)

Introduction:

Agriculture is universally recognized as a cornerstone of human existence, significantly influencing the economy [1]. Monitoring agricultural areas is crucial for addressing global challenges such as rising food demand driven by population growth and climate change [2]. Accurate crop classification is essential for estimating crop production, with timely and precise information on crop types being in high demand [3][4]. To tackle these issues, both spatial and temporal data on crop distribution are required. Remote sensing is frequently employed to map crop distribution efficiently on a global scale [5]. Multi-spectral and multi-temporal remote sensing data are utilized to create crop maps, demonstrating their capability to assess vegetation status over time [6]. Traditionally, crop-type classification has relied heavily on single-source optical satellite data. However, the increasing acceptance of multi-source satellite imagery reflects advancements in sensor technology and processing power. In the realm of crop type classification, combining optical and radar data is particularly advantageous as it leverages the strengths of both sensor types [7]. Sentinel-2 data provides a unique combination of high spectral and spatial resolution with a short revisit period of 5 days. Meanwhile, Sentinel-1 (SAR) data meets the stringent requirements for effective crop monitoring. SAR data's frequency and polarization offer superior insights into topography, soil moisture, roughness, and canopy structure, even under cloud cover [8]. Optical data, on the other hand, utilizes electromagnetic radiation in the visible, near-infrared, and shortwave infrared ranges to provide vital information on moisture content, leaf colors, and overall vegetation health [9]. Combining multiple sensors with various spatial and temporal resolutions can enhance data availability and accuracy [10]. Spectral bands from multi-spectral time-series data, along with vegetation indices such as NDVI, NDWI, NDMI, and BSI, have been used to improve crop type classification accuracy [11].

The pixel-based approach to integrating Sentinel-1 and Sentinel-2 data often suffers from the salt-and-pepper effect in classification results, which can undermine the integrity of crop field analysis [12][13]. Image segmentation technology divides an image into numerous segments, and many studies have highlighted that segmentation methods like Simple Non-Iterative Clustering (SNIC) offer a promising alternative to traditional pixel-based classification techniques. SNIC, being a highly advanced super-pixel segmentation algorithm, is noted for its speed and low memory consumption, making it highly suitable for crop mapping [14][15]. Machine learning techniques, such as Random Forest (RF), can further enhance crop type identification [16]. RF is a widely used classifier known for its accuracy and efficiency [17], often outperforming other classifiers [18]. While Support Vector Machine (SVM) is also a competent classifier, it can be more complex due to the need for selecting and tuning various input parameters and kernels [19]. Most classification techniques rely on high-quality training data and appropriate feature combinations, which significantly impact the consistency of classification outcomes [20].

Recent studies have conducted comparative analyses of Pixel-Based and Object-Based Algorithms, utilizing integrated Sentinel-1, Sentinel-2, and NDVI Data on Google Earth Engine (GEE) for crop identification. GEE, as a cloud computing platform, facilitates the automation of crop classification techniques. This study aims to compare pixel-based and object-based approaches by employing machine learning algorithms such as Random Forest (RF) on the integration of time series data from Sentinel-1, Sentinel-2, and NDVI. The primary objective is to assess the effectiveness of the object-based segmentation approach (using GEE and E-Cognition) versus the pixel-based approach in classifying cotton, rice, and sugarcane.

Objectives:

Specifically, the study aims to achieve three main objectives:

- To illustrate how integrating Sentinel-1 and Sentinel-2 data can improve classification accuracy.
- To assess the accuracy of crop type identification using machine learning algorithms, such as Random Forest (RF).
- To compare the accuracy of crop classification using pixel-based versus object-based approaches, including the application of the Simple Non-Iterative Clustering (SNIC) algorithm, utilizing Google Earth Engine (GEE).

Material and Methods:

Study Area:

Rahim Yar Khan, a prominent city in southern Punjab, Pakistan, spans an area of 11,880 square kilometers, constituting 5.79% of Punjab's area and 1.4% of Pakistan's total area. It is located along the banks of the River Indus and is divided into four Tehsils. The city lies between latitudes 27° 56' and 28° 52' N and longitudes 70° 00' and 70° 32' E. The climate of the area is classified as arid subtropical continental, with a mean annual rainfall of 97.2 mm, predominantly occurring during the late summer monsoon season. Summer temperatures average 33.6°C, reaching daily maxima of 40.3°C, while winter temperatures average 14.5°C, with daily minima of 5.7°C. A map of the study area and its location within Punjab, Pakistan, is shown in Figure 1.

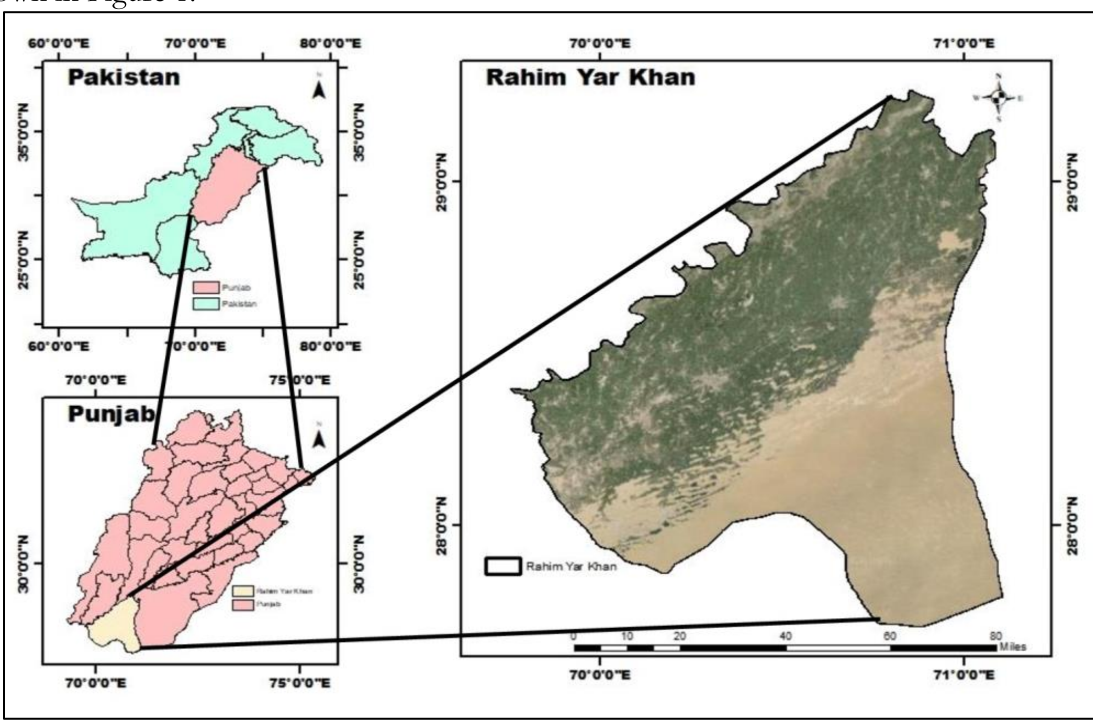

Figure 1: Study Area Map of Rahim Yar Khan in Punjab, Pakistan.

Analysis Framework:

The overall methodology employed in this study is illustrated in Figure 2.

Field Survey Data:

Field information, or ground truth data, were gathered through GPS and visual observation. This data collection took place in Rahim Yar Khan during August and September 2019. The major crops identified were sugarcane, rice, and cotton, while other land-use classes included orchards, built-up areas, barren land, water bodies, and other crops. Field sample points were recorded with GPS and photographic evidence during the Kharif season. Seventy percent of these points were used for classification purposes, while the remaining thirty percent were reserved for validation. The latitude and longitude of each sample were also documented. The distribution of all field sample points is shown in Figure 3.

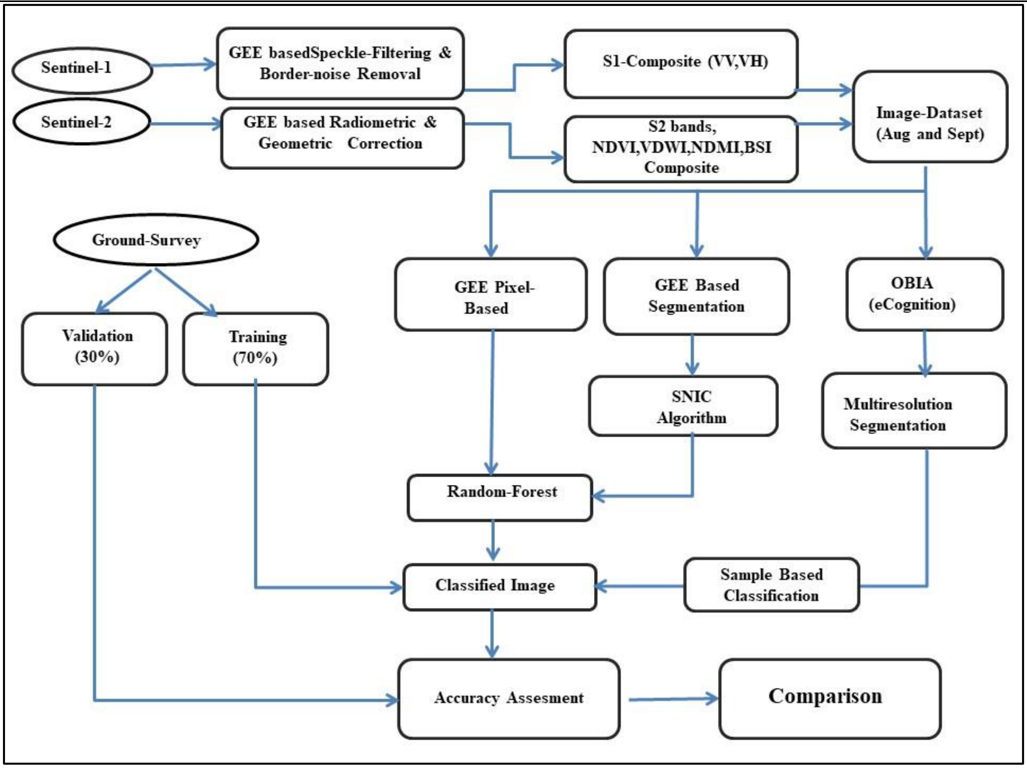

Figure 2: Methodological Flow Chart of the Study

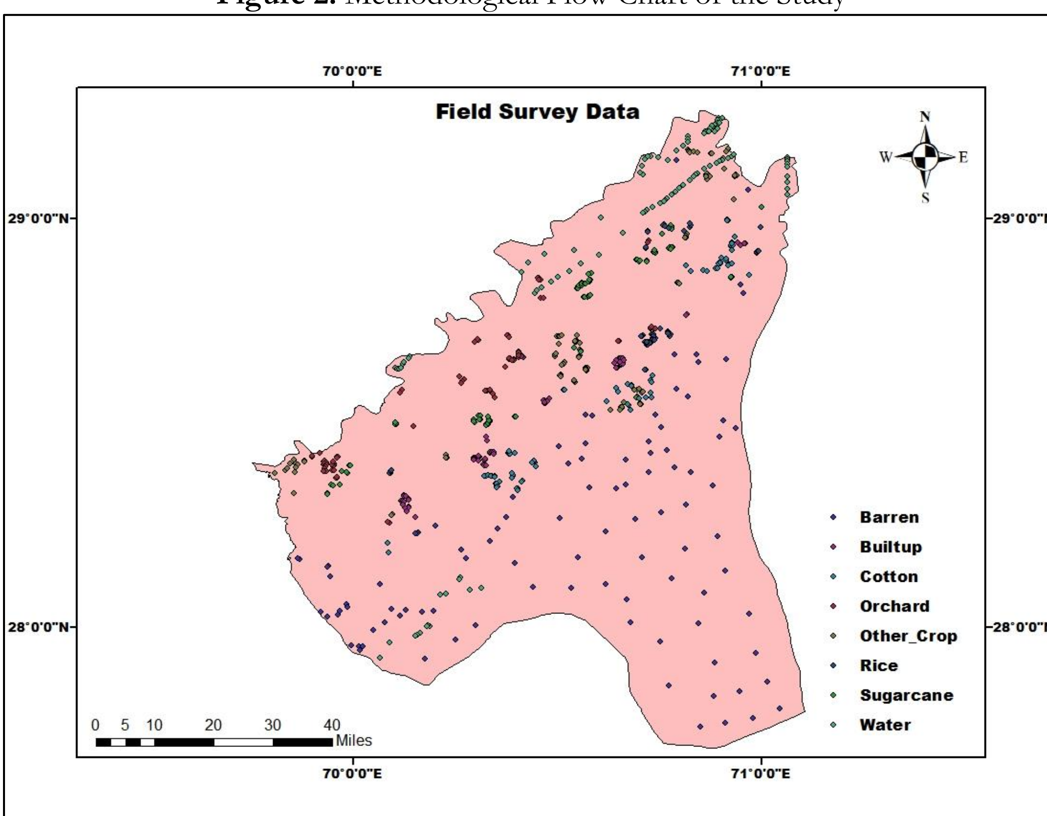

Figure 3: Field Sample Points of Cotton, Rice and Sugar Cane taken from all over the Study Area

Image Datasets and Pre-Processing:

Sentinel-1 and Sentinel-2 satellite data highlight the significance of crop classification, particularly in regions experiencing rapid changes [21]. In this study, Synthetic Aperture Radar

(SAR) images from Sentinel-1 and optical images from Sentinel-2 were utilized. These sensors were selected primarily due to their availability and cost-free access. Both temporal, spectral, and spatial resolutions of the data were accessed via the Google Earth Engine (GEE) platform. Sentinel-1, operating in the C-band SAR, provides multiple imaging modes with resolutions ranging from 10 to 60 meters. The S1_GRD dataset of Sentinel-1 was employed, which emits microwave signals to capture reflected energy, resulting in SAR images based on signal delays. These images are valuable for monitoring Earth's surface changes and are usable in all weather conditions. Overall, Sentinel-1 SAR is essential for environmental, disaster, and scientific applications [22].

Sentinel-2 data also played a crucial role in this study. Sentinel-2A features 13 bands with wavelengths ranging from 443 to 2190 nm and high-resolution optical sensors with spatial resolutions of 10 m, 20 m, and 60 m, as detailed in Table 1. The Sentinel-2 bands used in this study are listed in Table 2. Specifically, bands B08 and B04 were employed to calculate the Normalized Difference Vegetation Index (NDVI) as shown in Equation 1, bands 8A and B11 were used to compute the Normalized Difference Water Index (NDWI) as shown in Equation 2, bands B08 and B11 were utilized for the Normalized Difference Moisture Index (NDMI) as shown in Equation 3, and bands B11 and B04 were used to derive the Bare Soil Index (BSI) as shown in Equation 4. These indices, combined with Sentinel-2 bands, were used to enhance the classification process [11].

Table 1: General Specification of Sentinel-1 and Sentinel-2.

Description	Sentinel-1 (SAR)	Sentinel-2
Resolution	10 m	10,20 ,60m
Band Type	C-Band	Coastal Aerosol, Blue, Green, Red, NIR and SWIR
Revisit Time	6 days	5 Days
Orbit Height	693km	786km
Orbit Inclination	98.18^0	98.63^0
Spectral Range	3.75-7.5cm	0.44-2.19μm

Table 2: Sentinel-2 bands utilized in this study.

Band Number	Sentinel-2 Bands	Central Wavelength(nm)	Spatial Resolution(m)
Band 2	Blue	490	10
Band 3	Green	560	10
Band 4	Red	665	10
Band 5	Red Edge	705	20
Band 6	Red Edge	740	20
Band 7	Red Edge	783	20
Band 8	NIR	842	10
Band 8A	Red Edge	865	20
Band 11	SWIR	1610	20
Band 12	SWIR	2190	20

$$\mathrm{NDVI} = \frac{B08-B04}{B08+B04} \quad (1)$$

$$\mathrm{NDWI} = \frac{B8A-B11}{B8A+B11} \quad (2)$$

$$\mathrm{NDMI} = \frac{B08-B11}{B08+B11} \quad (3)$$

$$\mathrm{BSI} = \frac{B11-B04}{B11+B04} \quad (4)$$

The initial step involves acquiring and pre-processing satellite imagery datasets from Sentinel-1 and Sentinel-2 platforms using Google Earth Engine (GEE). For Sentinel-1 data, images were selected based on crop growth periods (e.g., August 2019 for cotton, September 2019 for rice and sugarcane), and included VV and VH polarizations, Interferometric Wide (IW) mode, and both ascending and descending orbits to ensure comprehensive imaging. After retrieval, each Sentinel-1 image undergoes pre-processing to enhance data quality. This includes removing border noise to improve accuracy by masking areas with incorrect or missing data and applying speckle filtering using a focal median filter to reduce noise effects and enhance image clarity.

Following the processing of Sentinel-1 data, Sentinel-2 data was filtered based on crop phenology periods, with a focus on images exhibiting less than 20% cloud cover. Pre-processing included cloud masking using the Quality Assessment (QA) band, as well as geometric and radiometric correction. Radiometric correction adjusts satellite imagery to accurately reflect surface properties, accounting for sensor and atmospheric effects. Geometric correction aligns images to eliminate spatial distortions caused by Earth's curvature and sensor orientation, ensuring accurate spatial analysis and map overlay. Additionally, pre-processing involved computing indices such as NDVI, NDWI, NDMI, and BSI, clipping images to the study area, and averaging band values across the date range to enhance data consistency.

After pre-processing both datasets, the mean images were stacked to create a composite image. This composite integrated data from Sentinel-1 (VV and VH bands), Sentinel-2 (selected spectral bands), and the computed indices. This process was applied for the months of August 2019 (for cotton) and September 2019 (for rice and sugarcane), as detailed in Table 3.

Table 3: Composite Image Dates for Classification of Crop-Type.

Crop-Type	Start-Date	End-Date
Cotton	01-08-2019	30-08-2019
Rice & Sugarcane	01-09-2019	30-09-2019

This unified representation improves the accuracy of crop classification analyses. Ultimately, the stacked image is visually presented on a map to facilitate interpretation and analysis.

Google Earth Engine Based Classification:

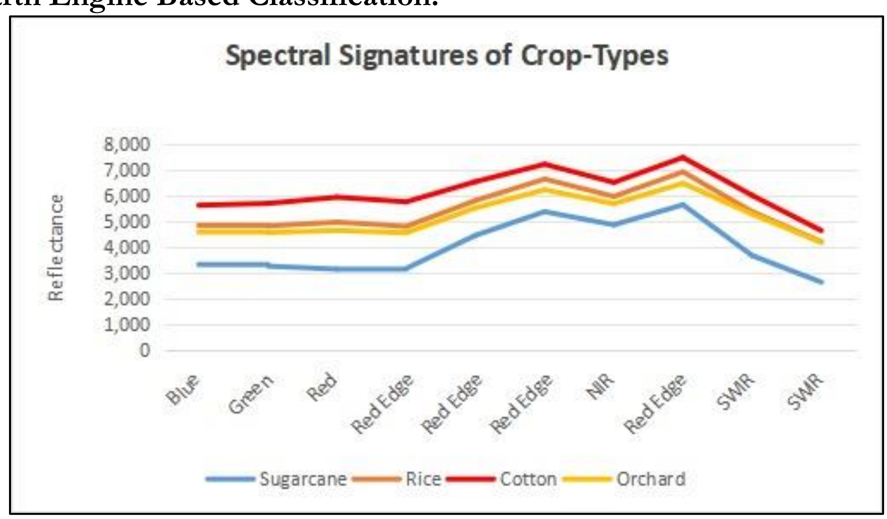

Figure 4: Spectral-Signatures of Different Crop Classes

Sentinel-1 SAR and Sentinel-2 image data were acquired through Google Earth Engine, followed by pre-processing steps for both datasets. For Sentinel-1 data, speckle filtering and border noise removal were applied. Sentinel-2 data underwent radiometric and geometric corrections, and NDVI indices were derived from this dataset. After pre-processing, reducers were applied to the Sentinel-1 and Sentinel-2 data, as well as the indices. Composite images were then created by integrating Sentinel-1, Sentinel-2, and NDVI data, and the images were clipped to the study area. Pixel-based and object-based classifications were performed using the Random Forest algorithm on the integrated data. For object-based classification, the Simple Non-Iterative Clustering (SNIC) algorithm was utilized within Google Earth Engine (GEE). E-Cognition was employed for multi-resolution segmentation and Object-Based Image Analysis (OBIA). Accuracy assessments of the three classification methods were conducted using a confusion matrix to calculate overall accuracy, producer accuracy, and Kappa. The classification process involved a thorough evaluation of spectral classes for different crop types using various Sentinel-2 bands, with the Red Edge band proving especially useful for distinguishing crop types. The spectral signatures for all crop fields in Sentinel-2 imagery are shown in Figure 4.

SNIC Image Segmentation:

The traditional pixel-based classification technique often results in "salt and pepper" noise. To address this, the object-based approach uses neighboring pixel information to segment the image into distinct regions or objects based on specific parameters, thereby reducing such noise. In this study, the Simple Non-Iterative Clustering (SNIC) image segmentation technique in Google Earth Engine (GEE) was employed [23]. The process begins with initializing centroid pixels on a regular grid across the image. Then, each pixel's distance from the centroid is measured in a five-dimensional space of color and spatial coordinates. This distance measurement enables the creation of efficient, compact, and nearly uniform polygons by integrating normalized spatial and color distances [24]. Key parameters of the SNIC algorithm include "image," "size," "compactness," "connectivity," "neighborhood size," and "seeds."

The "size" parameter determines the spatial extent of super-pixels or segments within the image. Larger sizes produce fewer but larger segments, while smaller sizes result in more but smaller segments. The "compactness" parameter controls the shape of the segments, affecting how closely they adhere to regular shapes like squares. Higher compactness values lead to more regular, compact segments, whereas lower values allow for more irregular shapes. The "connectivity" parameter defines how neighboring pixels influence each other during segmentation. A value of 4 indicates 4-connectivity, where pixels are connected horizontally and vertically, while 8-connectivity includes diagonal connections as well. The choice between 4 and 8 connectivity depends on the spatial arrangement of features in the imagery. The "seeds" parameter specifies the initial seed points from which the segmentation process begins, which is particularly relevant when object shapes vary significantly within the image.

In this study, the term "image" refers to the data used for segmentation. Integrated Sentinel-1, Sentinel-2, and NDVI time series images with different time intervals were used, specifically from 01-08-2019 to 30-08-2019 for cotton, and from 01-09-2019 to 30-09-2019 for rice and sugarcane. Segmentation sizes of 5, 10, 15, and 20 were tested, with size 15 yielding the best classification accuracy. The optimal neighborhood size was determined to be 128. Since the majority of parcels in the study area are rectangular, the "compactness" parameter was set to 0, and "connectivity" was evaluated at both 4 and 8. Given that the research area predominantly consists of rectangular portions, no specific "seeds" were established.

Random Forest:

The Random Forest (RF) algorithm, a powerful non-parametric machine learning classifier developed by [22], is widely employed in crop classification. RF utilizes bootstrap aggregation (bagging) to generate multiple decision trees, which are then aggregated through majority voting to enhance prediction accuracy. Its non-parametric nature, minimal generalization errors, and robustness to noise make it well-suited for crop classification tasks. Additionally, RF's ability to handle high-dimensional remote sensing data and identify key variables contributes to its popularity [25]. The RF classification algorithm is available on the Google Earth Engine (GEE) platform. In this study, the RF classifier was trained using training data, and classification accuracy was evaluated with verification data. Two key parameters were adjusted: the minimum size of a terminal node (min leaf) and the number of decision trees generated per class. Crop classification was performed with various settings for these parameters, and the optimal configuration was selected based on overall classification accuracy [26]. The number of features was set to the square root of the total number of features, and the number of trees was set to 100.

OBIA Multi-Resolution Segmentation:

Object-Based Image Analysis (OBIA) technology segments large images into smaller, homogeneous image objects based on their properties through a segmentation process. Unlike pixel-based methods, OBIA can incorporate additional properties such as spectral, shape, and texture information. Accurate segmentation is a critical step in object-oriented image processing, as it significantly influences the performance of object-based algorithms [27]. In this study, multi-resolution segmentation was applied using E-Cognition, with varying scales (30, 70, 90, 120) and levels of compactness (0.5) and shape (0.3, 0.5, 0.8). This advanced segmentation technique was employed to enhance the accuracy of object-based crop classification. By adjusting these parameters, we refined the segmentation process, resulting in more precise delineation of crop fields. This approach notably improved the accuracy of object-based classification, demonstrating the advantages of combining sophisticated segmentation tools with Random Forest for optimal crop mapping results.

Confusion Matrix and Accuracy Assessment:

In this study, cross-validation was employed to assess the model's performance. This process involved dividing the datasets into training and validation sets, with a portion of the training data reserved for testing the model's parameters. The model's performance was evaluated on the validation dataset to determine its generalization capability. Specifically, the datasets were split into 70% for training and 30% for validation. After classification, the model's accuracy was analyzed using a confusion matrix and assessed with the kappa coefficient for consistency. The confusion matrix provides an organized comparison of reference and map data for computation. Qualitative evaluation of the classification results was conducted through image comparison, while quantitative assessment was achieved using statistical methods like the kappa coefficient and confusion matrix [22]. Overall Accuracy (OA) represents the proportion of correctly classified pixels, while the Kappa coefficient measures classification accuracy by accounting for chance agreement between prediction and reference data. Producer Accuracy (PA) indicates the proportion of correctly classified pixels within a reference class, and User Accuracy (UA) reflects the likelihood of correctly classifying a specific labeled sample. Producer accuracy, user accuracy, and overall accuracy were calculated to provide a comprehensive assessment of the model's performance.

Table 4: Accuracy Assessment of Land-Cover Classes by using field data validation points.

Land-Cover	OA	PA	UA	Kappa	F-Score
PB-Cotton	0.9809	0.6187	0.6113	0.9207	0.6150
OB-Cotton	0.9667	0.9671	0.9684	0.9587	0.9677
OBIA-Cotton	0.8508	0.8245	0.8254	0.8023	0.8167
PB-R&S	0.9696	0.7493	0.7590	0.9083	0.7541
OB-R&S	0.9411	0.9291	0.9531	0.9241	0.9409
OBIA-R&S	0.8911	0.8543	0.8623	0.8743	0.8832

Result and Discussion:

The classification accuracy of integrating Sentinel-1, Sentinel-2, and NDVI data using the Random Forest algorithm was evaluated for both pixel-based and object-based approaches, as shown in Table 4. The pixel-based approach achieved an overall accuracy and kappa of 0.9809 and 0.9696 for cotton, and 0.9207 and 0.9083 for rice. The object-based approach achieved an overall accuracy and kappa of 0.9667 and 0.9411 for cotton, and 0.9587 and 0.9241 for rice. The OBIA approach resulted in an overall accuracy and kappa of 0.8508 and 0.8543 for cotton, and 0.802 and 0.8743 for rice. The object-based classification using the SNIC approach produced better results compared to the pixel-based classification in Google Earth Engine and the OBIA in E-Cognition Developer. Despite all approaches yielding strong results due to the integration of SAR and optical data, the final output maps for each method are presented in Figures 5 and 6.

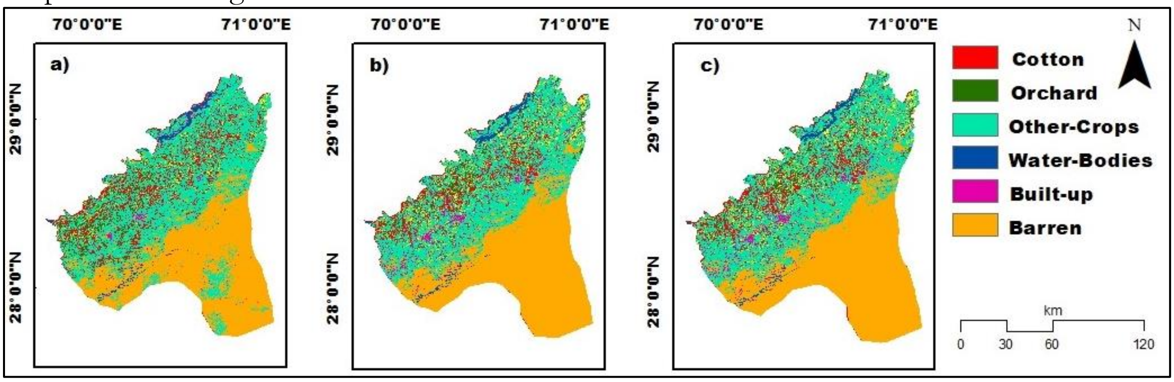

Figure 5: Classification maps for the image acquired in August (kharif crops focusing on Cotton) using the three different approaches; a) pixel-based using Random Forest classifier Google Earth Engine, b) object-based using Simple non iterative clustering SNIC and Random Forest classifier in Google Earth Engine, c) object-based using Multi-resolution segmentation and Nearest Neighbor classifier in e-Cognition

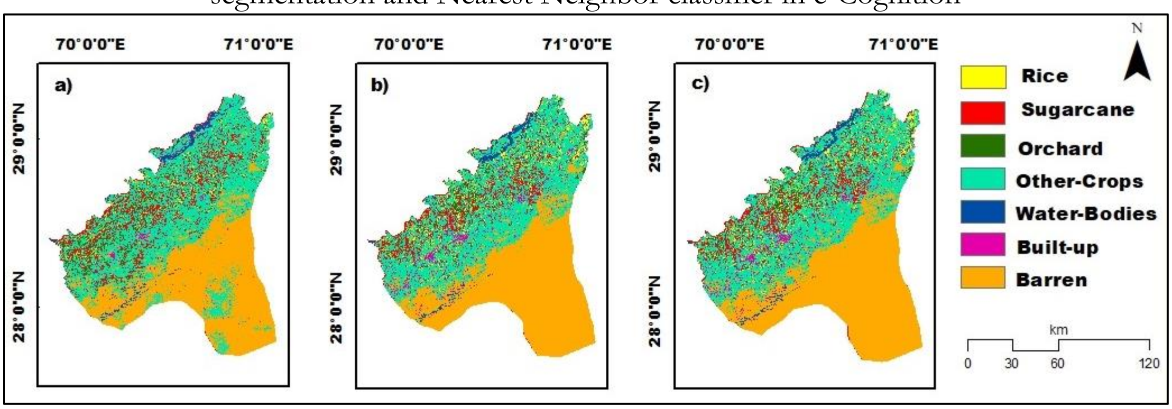

Figure 6: Classification maps for the image acquired in September (kharif crops focusing on Rice and Sugarcane) using the three different approaches; a) pixel-based using Random Forest classifier Google Earth Engine, b) object-based using Simple Non-Iterative Clustering SNIC and Random Forest classifier in Google Earth Engine, c) object-based using Multi-resolution segmentation and Nearest Neighbor classifier in e-Cognition

This study examined the comparative efficiency of pixel-based and object-based approaches for classifying cotton and rice, utilizing machine learning algorithms like Random Forest (RF) on integrated Sentinel-1, Sentinel-2, and indices such as NDVI, NDWI, NDMI, and BSI data within Google Earth Engine (GEE). The findings reveal notable differences in performance between the pixel-based and object-based methods, highlighting the strengths and limitations of each approach.

The pixel-based approach achieved high overall accuracy for both cotton (0.9809) and rice (0.9696). However, the producer's accuracy (PA) and user's accuracy (UA) for cotton were notably lower (0.6187 and 0.6113, respectively), suggesting that while the pixel-based method was effective for general classification, it struggled with accurately identifying cotton pixels. This discrepancy indicates potential issues with misclassification and the difficulties of using a pixel-based method to capture the variability of agricultural landscapes.

In contrast, the object-based approach demonstrated high accuracy, particularly for cotton, with an overall accuracy (OA) of 0.9667 and a Kappa of 0.9587. PA and UA for cotton were around 0.97, reflecting robust classification performance. For rice, the object-based method also performed well, with an OA of 0.9411 and a Kappa of 0.9241, along with high PA and UA values (0.9291 and 0.9531, respectively). These results underscore the object-based approach's ability to capture the spatial characteristics of the landscape by considering groups of pixels (objects) rather than individual pixels, which helps reduce noise and improve the definition of crop boundaries in heterogeneous agricultural areas.

While the object-based approach in GEE produced good results, it did not match the performance of the OBIA method. The SNIC approach attained an OA of 0.9667 and a Kappa of 0.9587 for cotton, with PA and UA around 0.9671 and 0.9684. For rice, SNIC results were lower, with an OA of 0.9411 and a Kappa of 0.9241, and PA and UA values of 0.9291 and 0.9531, respectively. Although OBIA is effective, its slightly lower performance compared to the object-based approach suggests that while segmentation improves classification, the specific methodology and tools used can significantly impact results. The object-based approach achieved high overall accuracy and a Kappa of 0.9677 and 0.9589, compared to OBIA's overall accuracy and Kappa of 0.8911 and 0.8743. Our results indicate that pixel-based approaches with different bands and indices produced better results than segmentation alone, though fine-tuning data is crucial. We recommend using a trial-and-error method when selecting segment size and compactness, as these parameters significantly affect results. While the pixel-based approach offers better overall control, segmentation results depend on the quality of segments created and the accuracy of the samples used for classification.

Discussion:

The results of this research corroborate recent studies emphasizing the advantages of integrating advanced classification techniques with multi-source satellite data for enhanced agricultural monitoring. The object-based approach demonstrated superior performance compared to pixel-based methods, particularly when utilizing the SNIC algorithm within Google Earth Engine (GEE). This finding aligns with research conducted by [28][29], which highlighted that analyzing groups of pixels (objects) rather than individual pixels significantly reduces noise and improves classification accuracy.

The object-based technique for classifying rice and cotton achieved high kappa values and overall accuracy, underscoring its effectiveness in capturing the spatial characteristics of crops. This is consistent with [30], who found that object-based approaches markedly improve crop boundary identification in varied agricultural settings. The object-based strategy in GEE outperformed the OBIA approach, illustrating the impact of processing platforms and segmentation methods on classification outcomes. Recent work by [31] emphasizes the importance of selecting appropriate platforms and segmentation parameters to achieve optimal results, noting that while OBIA offers advantages, the accuracy of segmentation and training samples are crucial for its effectiveness.

The study also identified limitations, such as classification errors and poor data quality, which are common challenges in remote sensing applications. Misclassification likely resulted from mixed pixels and variability in crop growth stages, a finding consistent with [26], who reported similar issues in agricultural classification. Additionally, the integration of optical data (Sentinel-2) with SAR data (Sentinel-1) proved beneficial, as supported by [29], who found that combining these complementary data sources enhances classification robustness and accuracy. Future research could address these limitations by exploring advanced machine learning techniques and incorporating new data sources, such as hyperspectral imagery or drone-based observations. Employing deep learning methods, as suggested by [32], could further improve the management of complex agricultural landscapes. Overall, this study highlights the potential for enhancing crop classification accuracy through advanced algorithms and multi-source satellite data, providing valuable insights for agricultural management and policy-making.

Conclusion:

Overall, integrating Sentinel-1, Sentinel-2, and composite images based on indices such as NDVI, NDWI, NDMI, and BSI proved advantageous across both pixel-based and object-based approaches. The object-based approach in Google Earth Engine (GEE), utilizing the SNIC algorithm, outperformed both the pixel-based method and the OBIA approach with multi-resolution segmentation in e-Cognition Developer. This superiority is likely attributed to the superior handling of spatial information and the reduction of classification noise. While the pixel-based method achieved high overall accuracy, its lower producer and user accuracy values highlight its limitations in heterogeneous landscapes. Although the OBIA method was useful, it did not match the accuracy of the object-based method in GEE, underscoring the importance of advanced segmentation techniques for enhancing classification precision.

These findings underline the necessity of selecting classification methods based on the specific needs and characteristics of the study area. Future research should focus on refining object-based methods, particularly in the context of integrating multi-source remote sensing data, to further improve classification accuracy and reliability in complex agricultural environments.

Acknowledgements: I would like to express my sincere gratitude to the Urban Unit for their significant contribution to this research by providing ground survey data for crops in Rahim Yar Khan. I also extend my appreciation to the European Space Agency for granting access to Sentinel-1 and Sentinel-2 satellite imagery and to Google Earth Engine for its crucial role in crop analysis and classification.

Author's Contribution: All the authors had different contributions to this research work and are mentioned here accordingly. Conceptualization (A.S, S.M.I, M.U), formal analysis (A.S., S.M.I, S.A), methodology (S.M.I, A.S, S.A), writing—original draft preparation (S.M.I, A.S, S.A), writing—review and editing (S.M.I, A.S, S.A,S.U.K,M.U), visualization (S.M.I, A.S, S.A,S.U.K,M.U) All authors have read and agreed to the published version of the manuscript.

Conflict of Interest: The authors declare that there is no conflict of interest regarding the publication of this manuscript in IJIST.

References:

[1] K. Ennouri, "Remote Sensing : An Advanced Technique for Crop," vol. 2019, 2019.

[2] K. Heupel, D. Spengler, and S. Itzerott, "ORIGINAL ARTICLE A Progressive Crop-Type Classification Using Multitemporal Remote Sensing Data and Phenological Information," PFG – J. Photogramm. Remote Sens. Geoinf. Sci., vol. 86, no. 2, pp. 53–69, 2018, doi: 10.1007/s41064-018-0050-7.

[3] D. Tilman, C. Balzer, J. Hill, and B. L. Befort, "Global food demand and the sustainable intensification of agriculture," Proc. Natl. Acad. Sci., vol. 108, no. 50, pp. 20260–20264, Dec. 2011, doi: 10.1073/pnas.1116437108.

[4] A. Shelestov, M. Lavreniuk, N. Kussul, A. Novikov, and S. Skakun, "Exploring Google Earth Engine Platform for Big Data Processing: Classification of Multi-Temporal Satellite Imagery for Crop Mapping," Front. Earth Sci., vol. 5, Feb. 2017, doi: 10.3389/feart.2017.00017.

[5] S. Murod, M. Ibra, A. Mustakim, and V. Du, "A crop type dataset for consistent land cover classification in Central Asia," pp. 1–6, 2020, doi: 10.1038/s41597-020-00591-2.

[6] A. Khaliq, L. Peroni, and M. Chiaberge, "Land Cover and Crop Classification using Multitemporal Sentinel-2 Images Based on Crops Phenological Cycle," 2018 IEEE Work. Environ. Energy, Struct. Monit. Syst., pp. 1–5, 2018.

[7] A. Orynbaikyzy, U. Gessner, and C. Conrad, "Crop type classification using a combination of optical and radar remote sensing data : a review," Int. J. Remote Sens.,

vol. 00, no. 00, pp. 1–43, 2019, doi: 10.1080/01431161.2019.1569791.
[8] E. Beriaux, A. Jago, C. Lucau-danila, V. Planchon, and P. Defourny, “Sentinel-1 Time Series for Crop Identification in the Framework of the Future CAP Monitoring,” pp. 1–29, 2021.
[9] A. Orynbaikyzy, U. Gessner, B. Mack, and C. Conrad, “Crop Type Classification Using Fusion of Sentinel-1 and Sentinel-2 Data : Assessing the Impact of Feature Selection , Optical Data Availability , and Parcel Sizes on the Accuracies,” 2020.
[10] G. Waldho, U. Lussem, and G. Bareth, “Int J Appl Earth Obs Geoinformation,” vol. 61, no. April, pp. 55–69, 2017, doi: 10.1016/j.jag.2017.04.009.
[11] G. R. Faqe Ibrahim, A. Rasul, and H. Abdullah, “Improving Crop Classification Accuracy with Integrated Sentinel-1 and Sentinel-2 Data: a Case Study of Barley and Wheat,” J. Geovisualization Spat. Anal., vol. 7, no. 2, pp. 1–15, 2023, doi: 10.1007/s41651-023-00152-2.
[12] L. Yang, L. R. Mansaray, and J. Huang, “Optimal Segmentation Scale Parameter , Feature Subset and Classification Algorithm for Geographic Object-Based Crop Recognition Using Multisource Satellite Imagery”, doi: 10.3390/rs11050514.
[13] E. O. Makinde, A. T. Salami, J. B. Olaleye, and O. C. Okewusi, “Object Based and Pixel Based Classification Using Rapideye Satellite Imager of ETI-OSA, Lagos, Nigeria,” Geoinformatics FCE CTU, vol. 15, no. 2, pp. 59–70, 2016, doi: 10.14311/gi.15.2.5.
[14] J. Brinkhoff, J. Vardanega, and A. J. Robson, “Land Cover Classification of Nine Perennial Crops Using Sentinel-1 and -2 Data,” pp. 1–26, 2020, doi: 10.3390/rs12010096.
[15] A. Paludo, W. R. Becker, J. Richetti, L. C. De, A. Silva, and J. A. Johann, “Mapping summer soybean and corn with remote sensing on Google Earth Engine cloud computing in Parana state – Brazil,” 2020, doi: 10.1080/17538947.2020.1772893.
[16] S. Ahmed, “Comparison of Satellite Images Classification Techniques using Landsat-8 Data for Land Cover Extraction,” Int. J. Intell. Comput. Inf. Sci., vol. 0, no. 0, pp. 1–15, 2021, doi: 10.21608/ijicis.2021.78853.1098.
[17] Y. Jin, X. Liu, Y. Chen, X. Liang, and Y. Chen, “Land-cover mapping using Random Forest classification and incorporating NDVI time-series and texture : a case study of central Shandong incorporating NDVI time-series and texture : a case study of central Shandong,” Int. J. Remote Sens., vol. 39, no. 23, pp. 8703–8723, 2018, doi: 10.1080/01431161.2018.1490976.
[18] V. F. Rodriguez-Galiano and M. Chica-Rivas, “Evaluation of different machine learning methods for land cover mapping of a Mediterranean area using multi-seasonal Landsat images and Digital Terrain Models,” Int. J. Digit. Earth, vol. 7, no. 6, pp. 492–509, Jul. 2014, doi: 10.1080/17538947.2012.748848.
[19] G. De Luca, M. N. Silva, S. Cerasoli, J. Campos, S. Di Fazio, and G. Modica, “Object-Based Land Cover Classification of Cork Oak Woodlands using UAV Imagery and Orfeo ToolBox,” 2019.
[20] Y. Wang, Z. Li, C. Zeng, G. Xia, and S. Member, “An Urban Water Extraction Method Combining Deep Learning and Google Earth Engine,” vol. 13, pp. 769–782, 2020.
[21] M. J. Steinhausen, P. D. Wagner, B. Narasimhan, and B. Waske, “Combining Sentinel-1 and Sentinel-2 data for improved land use and land cover mapping of monsoon regions,” Int. J. Appl. Earth Obs. Geoinf., vol. 73, pp. 595–604, Dec. 2018, doi: 10.1016/j.jag.2018.08.011.
[22] A. Moumni and A. Lahrouni, “Machine Learning-Based Classification for Crop-Type Mapping Using the Fusion of High-Resolution Satellite Imagery in a Semiarid Area,”

Scientifica (Cairo)., vol. 2021, pp. 1–20, Apr. 2021, doi: 10.1155/2021/8810279.
[23] R. Achanta and S. Sabine, "Superpixels and Polygons using Simple Non-Iterative Clustering," no. Ic, pp. 4651–4660.
[24] M. Mahdianpari, B. Salehi, and F. Mohammadimanesh, "The First Wetland Inventory Map of Newfoundland at a Spatial Resolution of 10 m Using Sentinel-1 and Sentinel-2 Data on the Google Earth Engine Cloud Computing Platform", doi: 10.3390/rs11010043.
[25] M. Vizzari, G. Lesti, S. Acharki, and M. Vizzari, "Geo-spatial Information Science Crop classification in Google Earth Engine : leveraging Sentinel-1 , Sentinel-2 , European CAP data , and object-based machine-learning approaches European CAP data , and object-based machine-learning approaches," Geo-spatial Inf. Sci., vol. 00, no. 00, pp. 1–16, 2024, doi: 10.1080/10095020.2024.2341748.
[26] E. Engine, "Accuracy Improvements to Pixel-Based and Object-Based LULC Classification with Auxiliary Datasets from Google Earth Engine," 2021.
[27] H. Gao, L. He, Z. wei He, and W. qian Bai, "Early landslide mapping with slope units division and multi-scale object-based image analysis — A case study in the Xianshui River basin of Sichuan, China," J. Mt. Sci., vol. 19, no. 6, pp. 1618–1632, 2022, doi: 10.1007/s11629-022-7333-6.
[28] Z. Ye et al., "A comparison between Pixel-based deep learning and Object-based image analysis (OBIA) for individual detection of cabbage plants based on UAV Visible-light images," Comput. Electron. Agric., vol. 209, no. April, p. 107822, 2023, doi: 10.1016/j.compag.2023.107822.
[29] T. Lu, M. Gao, and L. Wang, "Crop classi fi cation in high- resolution remote sensing images based on multi-scale feature fusion semantic segmentation model," no. August, pp. 1–16, 2023, doi: 10.3389/fpls.2023.1196634.
[30] S. Liu, Z. Qi, X. Li, and A. G. Yeh, "Integration of Convolutional Neural Networks and Object-Based Post-Classification Refinement for Land Use and Land Cover Mapping with Optical and SAR Data," pp. 1–25, 2019, doi: 10.3390/rs11060690.
[31] Q. Guo et al., "Urban Tree Classification Based on Object-Oriented Approach and Random Forest Algorithm Using Unmanned Aerial Vehicle (UAV) Multispectral Imagery," Remote Sens., vol. 14, no. 16, p. 3885, Aug. 2022, doi: 10.3390/rs14163885.
[32] H. Xue et al., "Object-Oriented Crop Classification Using Time Series Sentinel Images from Google Earth Engine," 2023.